

Lattice-Scale Domain Wall Dynamics in Ferroelectrics

Hongzhou Ma,¹ Won-Jeong Kim,² James S. Horwitz,³ Stephen W. Kirchoefer,⁴ and Jeremy Levy^{1,*}

¹*Department of Physics and Astronomy, University of Pittsburgh, 3941 O'Hara Street, Pittsburgh, Pennsylvania 15260, USA*

²*Department of Physics, Changwon National University, 9 Sarim-dong, Changwon 641-773, Korea*

³*Department of Energy, Basic Energy Sciences, Germantown, Maryland 20874-1290, USA*

⁴*Naval Research Laboratory, Washington, D.C. 20375, USA*

(Received 30 April 2003; published 20 November 2003)

Ferroelectric domain walls are atomically thin, and consequently their dynamics are sensitive to the periodic potential of the underlying lattice. Despite their central role in domain dynamics, lattice-scale effects have never been directly observed. We investigate local domain dynamics in thin film ferroelectrics using atomic-force microscopy. Upon combined dc and ac electric driving, fluctuations in the local piezoresponse are observed. Fourier analysis of the fluctuations reveals the presence of narrow band and broad band noise, and Barkhausen jumps. The narrow band noise is attributed to dynamics associated with lattice-scale pinning and is reproduced by a simple physical model.

DOI: 10.1103/PhysRevLett.91.217601

PACS numbers: 77.80.Dj

Nearly all of the interesting and useful properties of ferroelectrics can be traced back to the patterns and dynamics of domain walls, the boundaries that separate regions of uniform electric polarization [1]. Unlike magnetic domain walls, whose widths $\xi_M \sim 10\text{--}100$ nm are much larger than the lattice constant a , ferroelectric domain walls are atomically thin, with $\xi_E \geq a$. More than 50 years ago, Landauer noted [2] that since the domain wall is comparable in extent to the interatomic spacing [see Fig. 1(a)], it should be strongly pinned by the lattice itself (also known as the Peierls potential [3]). Domain motion can occur through thermal activation over the Peierls potential, and an applied electric field E can strongly influence the rate.

When a domain wall is driven externally, the periodic Peierls potential should in principle produce oscillations in the domain wall velocity, similar to “narrow band noise” in charge-density-wave (CDW) conductors [4] or the ac Josephson effect in superconductors [5]. All three physical systems can be represented abstractly by a single configurational coordinate s (i.e., domain wall displacement, CDW, or superconducting phase) subject to a global and periodic potential $U(s)$ [Fig. 1(b)].

Here we report what we believe to be the first direct observation of lattice-scale domain wall dynamics in a ferroelectric thin film. The measurements were conducted with an atomic-force microscope (AFM) used not for ferroelectric imaging [6] or poling [7], but rather as a sensitive microphone. The local, noninvasive nature of the measurement, combined with a sample that exhibits a low barrier for domain motion, has allowed these effects to be observed for the first time.

We concentrate on the mechanical noise associated with domain wall dynamics in ferroelectric thin films. A wide range of velocities for 180° domains have been observed experimentally, ranging from angstroms per second to centimeters per second [8], and the behavior

is in reasonable agreement with phenomenological models that invoke lattice pinning [9]. More recent investigations show that 180° domain dynamics in epitaxial thin films also proceeds via thermal activation over the Peierls potential [10]. Clamping by the substrate [11] is known to inhibit strongly the movement of 90° domains in thin films [12]. However, recent experiments have shown empirically that control over oxygen pressure during the growth and annealing of $(\text{Ba}, \text{Sr})\text{TiO}_3$ films can reduce the tetragonality, causing the films to become nearly cubic [13]. Two different films were investigated. Both consist of 500 nm thick $(\text{Ba}_{0.5}\text{Sr}_{0.5})\text{TiO}_3$ films grown by pulsed laser deposition on MgO substrates [14]. One sample was deposited at 50 mTorr O_2 pressure, while the second was deposited at 500 mTorr O_2 . Optical investigations of films grown under similar conditions indicate that the polarizations of both films are primarily

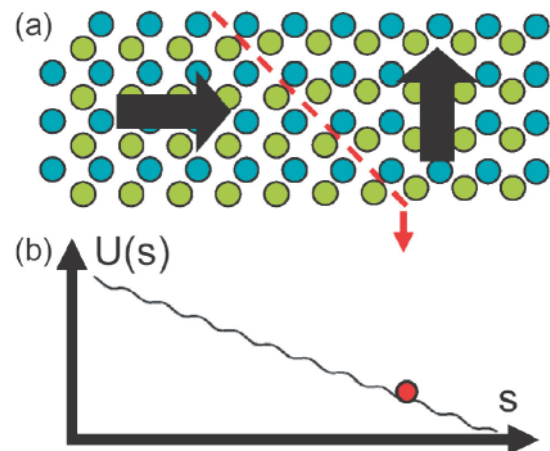


FIG. 1 (color online). (a) Lattice model of a 90° wall in a ferroelectric. (b) Sketch of energy function for the domain wall coordinate, showing the effects of an external field (overall slope) and atomic-scale periodicity.

out of plane oriented, and that applied in-plane electric fields can induce local reorientation of the ferroelectric polarization of the 50 mTorr film [15]. Interdigitated electrodes were deposited on top of the films, with a gap spacing between the electrodes $d = 10 \mu\text{m}$. More details about the growth and structural properties are described in Ref. [14].

Figure 2 shows a block diagram of the experimental arrangement. A home-built AFM with an insulating sharpened Si_3N_4 tip is used for topographic imaging and local measurements. The film is driven electrically using a balanced pair of voltage signals, so that the potential is always close to ground in the center of the film where the measurements are typically made. The AFM is operated in contact mode, and the vertical displacement of the cantilever is used to provide vertical feedback control. The piezoresponse of the film is measured by applying an in-plane dc + ac electric field $E(t) = E_{\text{dc}} + E_{\text{ac}} \cos(\omega t)$ and measuring the deflection of the cantilever using a standard optical bridge. The feedback set point is chosen to minimize nonpiezoelectric (e.g., electrostatic) contributions to the signal. Two lock-in amplifiers detect in-plane and out-of-plane deflections of the tip at the ac driving frequency $\omega/2\pi \sim 30 \text{ kHz}$.

Images of the sample topography and piezoresponse are obtained simultaneously by raster scanning the sample and recording the corresponding vertical height and lock-in signals. To minimize effects associated with thermal drift, several images are scanned in an interleaved fashion [16], using a repeating sequence of dc electric fields ($E_{d1}, E_{d2}, \dots, E_{dn}$) to acquire successive scan lines. Figures 3(a)–3(c) show representative images of the out-of-plane piezoresponse for the $P(\text{O}_2) = 50 \text{ mTorr}$ sample. Without a dc bias [Fig. 3(b)], the response at the driving frequency ω is nearly absent, providing strong evidence that the spontaneous polarization is primarily out of plane. Upon application of an in-plane

bias field [Figs. 3(a) and 3(c)], a distinct response is observed. Changes in the piezoresponse are associated with nanopolar reorientation of the ferroelectric polarization from out of plane to in plane.

The local piezoresponse can be obtained from this data set by averaging over a small area ($\sim 50 \text{ nm}$) and plotting the topographic response [Fig. 3(f)], in-phase [Fig. 3(d)], and out-of-phase [Fig. 3(e)] piezoresponses as a function of the applied electric field. For the data shown, a total of 14 interleaved images were taken, enough to illustrate the hysteretic response of the film. Changes in the film displacement, shown in Fig. 3(f), are approximately quadratic functions of the applied dc field, showing small but measurable hysteresis. The piezoresponse curves also exhibit hysteresis [Figs. 3(d) and 3(e)], indicative of domain motion, and the quadratic response is consistent with a predominantly out-of-plane polarization. The control sample [$P(\text{O}_2) = 500 \text{ mTorr}$] shows no hysteresis and a much weaker field-induced piezoresponse.

Investigations of fluctuations or noise in the piezoresponse [17] are obtained by fixing the tip at a single location on the sample, slowly ramping the dc electric field, and digitizing the time-dependent piezoresponse [18]. The qualitative features of the measured piezoresponse depend strongly on the amplitude of the ac driving. Two distinct regimes are observed [see Fig. 4(a)]. For low ac driving, the response is linear and rms fluctuations are small. Above a well-defined threshold ($\sim 2 \text{ kV}_{\text{rms}}/\text{cm}$), the response becomes nonlinear and fluctuations increase significantly. For Fig. 4(b), an ac amplitude $E_{\text{ac}} = 1 \text{ kV}_{\text{rms}}/\text{cm}$ was chosen. The dc field is slowly ramped

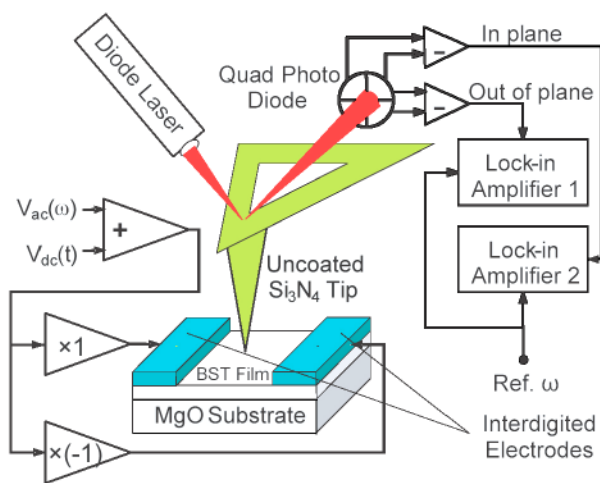


FIG. 2 (color online). Experimental arrangement.

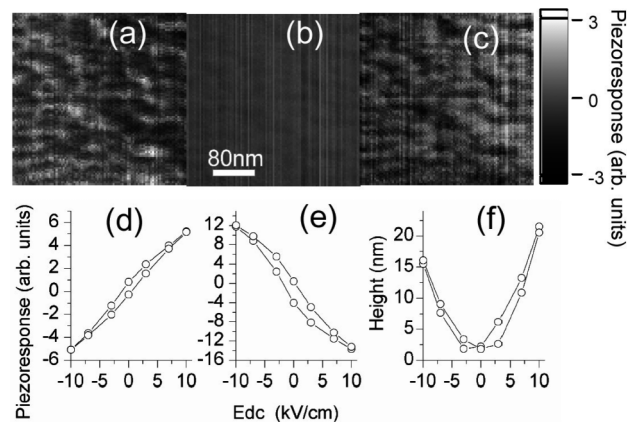


FIG. 3. Interleaved piezoresponse images of a $\text{Ba}_{0.5}\text{Sr}_{0.5}\text{TiO}_3$ thin film deposited in oxygen pressure $P(\text{O}_2) = 50 \text{ mTorr}$. A total 14 interleaved images are acquired at different dc electric fields E_{dc} , three of which are shown. The mean values of the image have been subtracted for clarity. (a) $E_{\text{dc}} = -10 \text{ kV/cm}$; (b) $E_{\text{dc}} = 0 \text{ kV/cm}$; (c) $E_{\text{dc}} = +10 \text{ kV/cm}$; (d)–(f) local hysteresis observed by averaging the interleaved images over a $50 \text{ nm} \times 50 \text{ nm}$ area. (d) In-phase piezoresponse. (e) Out-of-phase piezoresponse. (f) Hysteresis in the sample surface height.

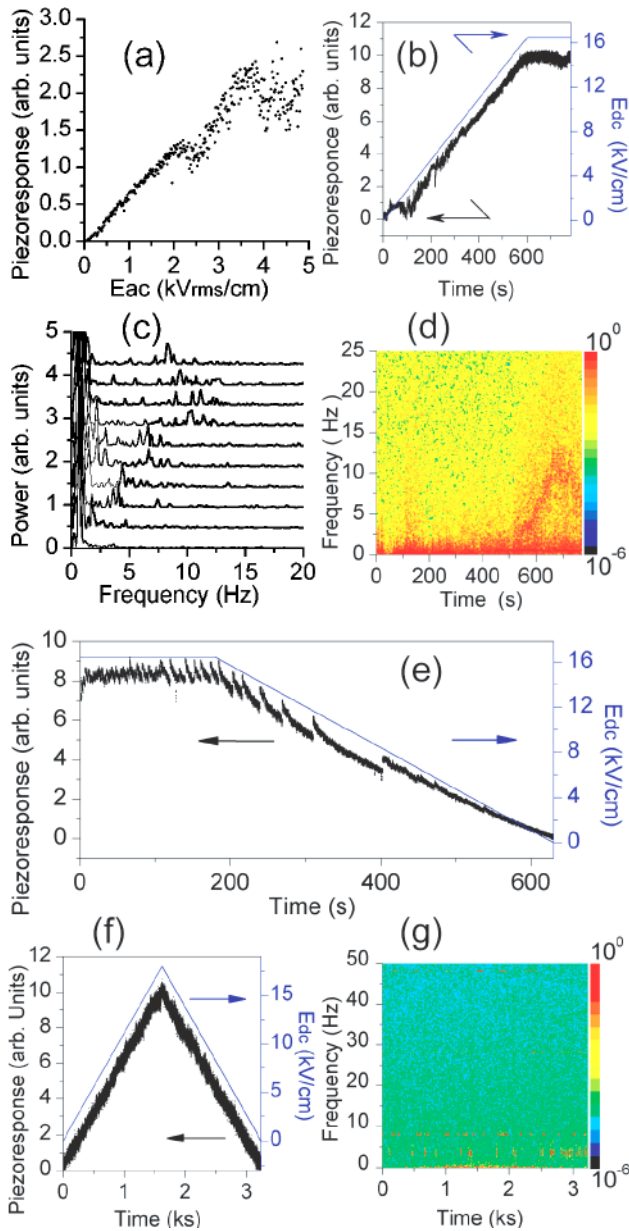


FIG. 4 (color online). Local noise measurements for $\text{Ba}_{0.5}\text{Sr}_{0.5}\text{TiO}_3$ grown at $P(\text{O}_2) = 50$ mTorr. (a) Piezoresponse versus ac amplitude. (b) Piezoresponse and dc bias versus time. (c) Fourier transform of temporal response at ten different times. (d) Intensity graph showing Fourier spectrum versus time. (e) Piezoresponse showing Barkhausen-type noise. (f) Piezoresponse and dc bias versus time for $\text{Ba}_{0.5}\text{Sr}_{0.5}\text{TiO}_3$ grown at $P(\text{O}_2) = 500$ mTorr. (g) Intensity graph showing Fourier spectrum versus time for $\text{Ba}_{0.5}\text{Sr}_{0.5}\text{TiO}_3$ grown at $P(\text{O}_2) = 500$ mTorr.

at a rate (27 V/cm s) and is kept constant for $600 < t < 800$ s, during which a corresponding change in the piezoresponse is observed.

To help analyze the response, a joint time-frequency analysis of the time series is performed, using a sweeping time interval of $T = 1.024$ s and Hanning windowing

[19]. The corresponding power spectra are displayed in a waterfall plot [Fig. 4(c)]. There is clear evidence of a well-defined “narrow band” noise over the interval shown, sustained over much of the time interval during which the dc field is held constant. Figure 4(d) shows an intensity plot of the noise spectra over the full time interval. The narrow band noise is clearly distinguished from lower frequency “broad band noise.” Its central frequency appears to be correlated with the applied dc bias, appearing only for bias fields above ~ 12 kV/cm. The highest center frequency is approximately 15 Hz, which is small compared to the driving frequency ω and large compared to the inverse waiting interval.

Narrow band noise has been observed in a number of locations on the sample, but not everywhere. The observation method is highly local, and noise is therefore expected to be observed only directly above a domain wall that is sufficiently mobile. Repeated experiments do not always produce the same noise signals, and the reason may be due to thermal drift (as much as 100 nm over the 13 min measurement interval).

The narrow band noise is distinct from Barkhausen jumps [20], also observed in this sample. Figure 4(e) shows typical Barkhausen jumps over the time interval $100 < t < 300$ s. The jumps are significantly larger in amplitude than the narrow band noise, and no Fourier transform is needed to discern them.

For the sample where $P(\text{O}_2) = 500$ mTorr, similar experiments and analyses were performed. For this sample, no discernible noise of any kind is observed [Figs. 4(f) and 4(g)]. That includes narrow band, broad band, and Barkhausen noise. The absence of narrow band noise for the control sample helps to rule out a large number of potential sources of artifacts for the observed effect.

The experimental results on the $P(\text{O}_2) = 50$ mTorr sample are consistent with the interpretation that fluctuations in the piezoresponse are associated with lattice-scale domain dynamics. This sample shows appreciable hysteresis, in contrast to the $P(\text{O}_2) = 500$ mTorr sample which exhibits no hysteresis and no fluctuations in the piezoresponse. The larger electro-optic response of films grown under conditions of low oxygen pressure is also consistent with this interpretation. What then are the physical mechanisms giving rise to the various types of noise observed? It is natural to ascribe the sudden and sometimes regular jumps in the measured piezoresponse to Barkhausen events [20]. The other sources of noise, broad band and narrow band, are more difficult to assign. The presence of both types is strongly reminiscent of behavior observed in sliding charge-density-wave conductors [4], which exhibit narrow band and broad band noise associated with the sliding of a periodic charge density over fixed defects in the crystal.

Here we propose a simple model to describe a physical mechanism for the narrow band noise. The dynamics of the domain wall coordinate s is presumed to be governed

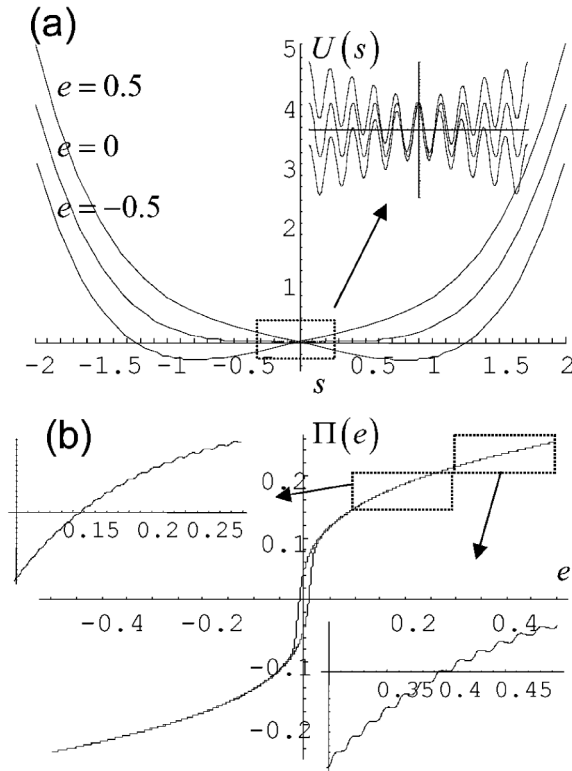


FIG. 5. One-dimensional model of ferroelectric domain wall to explain the origin of narrow band noise. (a) Solid curve represents Peierls potential at zero dc bias. Dashed curves represent the tilted potential when an external electric field is applied. The inset shows a close-up of the potential near $s = 0$. (b) Calculated piezoresponse as a function of dc bias, showing narrow band noise associated with lattice-scale domain wall dynamics.

by a one-dimensional potential: $U(s) = as^4 + (h/k) \times \cos(ks) - es$. The quartic term provides global confinement of the wall and is intended to model long-range effects of strain that are built up by the translation of 90° walls. The periodic lattice-scale Peierls potential is parametrized by a strength h and wave number k . An applied electric field e couples directly to the domain wall coordinate. Figure 5(a) displays a plot of $U(s)$ for three values of e . Domain wall dynamics are assumed to be overdamped, with a velocity given by $\dot{s} = -\nabla U(s)$. When a dc bias is applied, the potential is tilted, resulting in a displacement of the domain wall within the atomic-scale potential [21]. If the combined dc + ac field is large enough, the time-averaged Peierls barrier is lowered sufficiently to allow domain wall oscillation. The resulting piezoresponse is calculated by numerically simulating the domain dynamics and measuring the extent of domain

motion as a function of the dc electric field, as shown in Fig. 5(b). A close-up of the piezoresponse at large dc bias shows oscillations in the piezoresponse. Further analysis reveals that these oscillations correspond to domain wall amplitudes that alternate between n and $n + 1$ Peierls periods. That is, this model exhibits behavior that agrees qualitatively with the experimental results shown in Fig. 4.

This work was supported in part by the DARPA FAME program and the National Science Foundation (DMR-0333192). Discussions with Stephen Streiffer are gratefully acknowledged.

*Email address: jlevy@pitt.edu

- [1] M. E. Lines and A. M. Glass, *Principles and Applications of Ferroelectrics and Related Materials* (Clarendon, Oxford, 1977).
- [2] R. Landauer, *J. Appl. Phys.* **28**, 227 (1957).
- [3] R. E. Peierls, *Quantum Theory of Solids* (Oxford University Press, London, 1955).
- [4] G. Gruner, *Rev. Mod. Phys.* **60**, 1129 (1988).
- [5] B. D. Josephson, *Phys. Lett.* **1**, 251 (1962).
- [6] F. Saurenbach and B. D. Terris, *Appl. Phys. Lett.* **56**, 1703 (1990).
- [7] O. Kolosov *et al.*, *Phys. Rev. Lett.* **74**, 4309 (1995).
- [8] R. C. Miller and A. Savage, *Phys. Rev.* **115**, 1176 (1959).
- [9] R. C. Miller and G. Weinreich, *Phys. Rev.* **117**, 1460 (1959).
- [10] T. Tybell *et al.*, *Phys. Rev. Lett.* **89**, 097601 (2002).
- [11] S. Stemmer *et al.*, *J. Mater. Res.* **10**, 791 (1995).
- [12] F. Xu *et al.*, *J. Appl. Phys.* **89**, 1336 (2001).
- [13] C. Wontae *et al.*, *J. Appl. Phys.* **87**, 3044 (2000).
- [14] W. J. Kim *et al.*, *J. Appl. Phys.* **88**, 5448 (2000).
- [15] C. Hubert *et al.*, *Appl. Phys. Lett.* **79**, 2058 (2001).
- [16] R. M. Feenstra *et al.*, *Phys. Rev. Lett.* **58**, 1192 (1987).
- [17] Because the observed results for in-plane and out-of-plane responses are so similar, only results for the out-of-plane response are shown.
- [18] The lock-in amplifier (EG&G 5210) time constants were set to $TC = 1$ ms, with a 6 dB/octave, corresponding to an equivalent-noise bandwidth of 250 Hz. Most of the activity observed fell within 50 Hz, and hence a sampling interval of $Dt = 10$ ms was chosen.
- [19] A. V. Oppenheim, R. W. Schaffer, and J. R. Buck, *Discrete-Time Signal Processing* (Prentice Hall, Upper Saddle River, NJ, 1998).
- [20] A. G. Chynoweth, *Phys. Rev.* **113**, 159 (1959).
- [21] Thermal excitation over the Peierls barrier, known to be important for domain dynamics in real systems, is not included in this model.